


Article

Evaluating the Potential of Polylactide Nonwovens as Bio-Based Media for Air Filtration

Christina Schippers¹, Elena Marx¹, Ralf Taubner², Jochen S. Gutmann^{1,3} and Larisa Tsarkova^{1,4,*} ¹ German Textile Research Center (DTNW), 47798 Krefeld, Germany² Saxon Textile Research Institute (STFI), 09125 Chemnitz, Germany³ Physical Chemistry, University Duisburg-Essen and CENIDE, 45141 Essen, Germany⁴ Department of Chemistry, Moscow State University, 119991 Moscow, Russia

* Correspondence: tsarkova@dtnw.de

Abstract: The presented research aims to characterize hydrolytic resistance of highly crystalline and oriented polylactide (PLA) as a prerequisite for exploiting this bio-based material in durable applications. Industrially melt-spun PLA monofilaments and nonwovens have been subjected to environmental aging in a temperature range of 50–70 °C at a wide range of relative humidity (RH) in order to identify the onset of the material degradation under application conditions. Along with the measurements of mechanical and thermal behavior of the aged samples, the suitability of FTIR spectroscopy to probe the initial changes in the crystalline structure and in chemical composition of the fibers, caused by hydrolytic degradation, has been evaluated. The diagrams of stability and hydrolytic degradation under employed environmental aging for 7–14 days are presented for both types of PLA materials. Assessment of filtration performance of the artificially aged fibrous PLA media indicated a good agreement with the established stability diagram and confirmed the application potential of PLA nonwoven media, spun from currently available PLA grades, in air filtration under moderate climatic conditions up to max 50 °C and 50% RH. The presented results advance the knowledge on hydrolytic resistance of bio-based industry-relevant fibers and therefore open new application areas for sustainable materials with biodegradable components.

Keywords: bio-based polymers; polylactide; nonwoven filter media; PLA fibers; artificial aging; hydrolytic degradation



Citation: Schippers, C.; Marx, E.; Taubner, R.; Gutmann, J.S.; Tsarkova, L. Evaluating the Potential of Polylactide Nonwovens as Bio-Based Media for Air Filtration. *Textiles* **2021**, *1*, 268–282. <http://doi.org/10.3390/textiles1020014>

Academic Editor: Vincenzo Guarino

Received: 2 July 2021

Accepted: 3 August 2021

Published: 16 August 2021

Publisher's Note: MDPI stays neutral with regard to jurisdictional claims in published maps and institutional affiliations.



Copyright: © 2021 by the authors. Licensee MDPI, Basel, Switzerland. This article is an open access article distributed under the terms and conditions of the Creative Commons Attribution (CC BY) license (<https://creativecommons.org/licenses/by/4.0/>).

1. Introduction

Bio-based and biodegradable polylactide (PLA) is considered to be a perspective material to replace fossil-based polyethylene terephthalate (PET) in consumer goods and in technical textiles [1–5]. Nonwoven fabrics are manufactured from directionally or randomly oriented staple fibers or endless fibers via dry-/wet-laid or melt-spinning, respectively. To provide a mechanical integrity to the web, the fibers are bonded/entangled together mechanically, thermally or chemically [6]. Nonwovens offer an extended inner surface area in the form of a 3D network of fibers and the properties of textiles can be engineered to meet specific functions in the automotive industry, medical apparel [7], and filter media [8,9].

The separation efficiency of the nonwoven filters depends on morphology, surface characteristics, including charge storing ability (electret properties) of the fibers [10], and on the textile architecture, all predefined by the manufacturing process. Depth filters for industrial applications usually consist of several layers of nonwovens of different densities in order to be able to separate particles of several orders of magnitude within a single filtration stage. The fine-fiber nonwovens, which are capable of depositing the smallest substances (<0.4 µm in size), are produced using the meltblown process. In this single-stage production process, multiple single filaments are extruded at a nozzle tip, being strongly accelerated by means of converging hot air streams, and are stretched to small diameters up to a few µm [11].

Nonwovens, which are currently used in air filtration, are typically produced from petroleum-based thermoplastic polymers such as PET and polypropylene (PP). Although PLA is the only bio-based thermoplastic polymer, which is currently available in industrial amounts, it does not belong to so-called drop-in bioplastic such as bio-polyethylene, bio-PP or bio-PET. The latter bio-based polymers can be directly used with manufacturing processes and equipment developed for their fossil analogues. In contrast, processing of PLA as well as testing of the resulting PLA-based intrinsically degradable materials requires additional research input [12], including lifetime prediction models [13,14].

Numerous studies have established that PLA has specific physical properties, such as relatively low glass transition and melting temperatures [15], brittleness [16], slow crystallization behavior [17–19] as well as high hydrolytic and thermal instability [20–23], which make the resulting mechanical performance of the generated fibers sensitive to downstream processing steps as well as to the environmental conditions [24–29].

The mechanisms of hydrolytic degradation of PLA are well established [20,30,31], with the diffusion of water molecules being a limiting stage in case of bulk hydrolysis. Since the diffusivity and activity of water is smaller in the crystalline phase as in the amorphous phase, the degree of crystallinity of PLA has a greater influence than the degradation environment on the rate of hydrolysis [32], so that the degradation behavior of PLA depends on the molecular ordering imposed by the fabrication procedures.

In recent years, the processing and characteristics of meltblowns made from PLA have been studied with regard to their potential in filtration applications [8,9,33], including an assessment of the electret properties [34].

It should be noted, however, that the intrinsic thermal and hydrolytic degradability of PLA is a great challenge in designing PLA-based materials [30]. This concerns both the applications where a controlled degradation is promoted, e.g., in medical products such as implants and scaffolds [35], and the applications that require durable elastic-plastic deformation behavior rather than a brittle response at high stress levels. Numerous approaches to improve processability on the one hand and to control polymer properties on the other hand through, e.g., chemical modification of the polymer or blending, have been suggested [1].

An essential tool to improve the durability of PLA-based materials is to inhibit the hydrolytic degradation reaction. This can be achieved by slowing the diffusion of water molecules by intercalating nanoclays or graphene nanoplatelets, which create a physical barrier in the polymer matrix, through modifying the crystallinity of the material or by incorporating appropriate compounds (antihydrolysis agents) that react preferably with the polar end groups and/or with water [36]. However conventional approaches to toughen PLA via blending and reinforcement generally lead to a decrease in the initial strength of the material, and an identified challenge is to develop processing routes that can optimize the PLA structure to improve strength and ductility with or without incorporation of any other components.

Recent findings suggest that forcing the orientation of PLA nanocrystallites results in meso-morphic phases [37–39] that have enough long-term stability to enable the industrial use of PLA nonwovens in air filters at mild environmental conditions [29].

It has been shown that the molecular ordering of drawn-fibers from commercial-grade PLA strongly depends on the stereoregularity of the polymer and on the technological conditions applied during the fiber manufacturing process [24,27,40–42]. In particular, Puchalski et al. [26] have systematically characterized structural changes in the PLA and the content of crystalline meso-phases during the fabrication and bonding of PLA nonwoven fabric [27,42,43].

The scope of the present work concerns the possibility to engineer through the fabrication process and to predict application-specific degradation of PLA fibers. A balance between long-term stability and degradability is essential for a wide usage of industrial bio-based PLA materials.

In this paper, we consider a number of testing methods to assess the performance of artificially aged PLA monofilaments and melt-spun nonwovens, fabricated using industrial processing. Diagrams of stability against degradation are established, covering a wide range of potential application conditions with regard to temperature and humidity. We first present a methodological approach to assess the aging behavior of highly crystalline PLA monofilaments treated in a temperature range of 50–70 °C and in a range of relative humidity (RH) of 20–95% for two weeks. The methodology is then applied for nonwovens. Measurements of mechanical and thermal behavior of the treated monofilament and nonwoven samples, as well as FTIR spectroscopy, are presented. The accuracy of tensile stress measurements on fibrous textile materials is addressed. Finally, the filtration performance of the artificially aged media revealed a good agreement with the assessment of degradation using a combination of physical and chemical methods of analysis.

2. Materials and Methods

2.1. Raw Polymer Material

The raw materials used in this study for the preparation of nonwovens are commercial grades of PLA which are optimized for the intended processing: PLA Ingeo™ 6100D (Nature Works LLC, Minnetonka, USA), PLA Luminy® L130 (Total Corbion PLA, BA Gorinchem, Netherlands) and poly(butylene succinate) (PBS) grade BioPBS™ FZ71PM (PTT MCC Biochem Co. Ltd., Bangkok, Thailand). The two PLA grades are thermoplastic fiber-grade resins developed by respective providers for fiber processing using conventional spinning and drawing equipment. According to the providers' technical data sheets, the melting temperature T_m is ~165–180 °C and glass transition temperature T_g is ~55–60 °C. PBS was used as an additive (7%) for a production of some nonwoven samples to improve the flowing properties during the spinning. The technical data are available in respective data sheets of the provider.

2.2. Monofilament Preparation

Optically pure melt-drawn monofilaments were produced using industrial equipment at Monofil-Technik GmbH (Hennef, Germany), resulting in tough fibers with a glass transition temperature T_g of about 70 °C, degree of crystallinity of about 80% and an elastic modulus E of about 6.6 GPa [28], almost two times higher than reported values for the extruded materials and wet-spun fibers from commercial grade PLA of similar molecular weight [4]. The molecular weight M_w of the PLA in the fibers was about 120 kg/mol (measured with Gel Permeation Chromatography) and the fiber diameter, measured with an outside micrometer IP65 (Hogetex GmbH, Nieder-Olm, Germany) at multiple points, was 0.41 ± 0.01 mm.

2.3. Nonwoven Preparation and Characterization

The melt-spun nonwoven webs were prepared using a technological one-meter width pilot line Reicofil® 4.5 (Reifenhäuser Reicofil GmbH & Co. KG, Troisdorf, Germany). The large-scale downstream spinning block (block pressure 4000 bar) allows for higher degrees of molecular orientation and crystallization, as can be realized in processing using laboratory equipment. The randomly laid fibers on the conveyor belt, moving 37–45 m/min, were bonded into nonwoven sheets using hydro entanglement equipment, Aquajet, with three bands (90–110/185/185 bar) (Trützschler Nonwovens GmbH, Dülmen, Germany). In this process, fine water jets force the fibers to lock together. The entanglements occur when the water strikes the web and the fibers are deflected. The nonwoven characteristics are summarized in Table 1.

Table 1. Textile-technical parameters of nonwoven fabrics, evaluated according to corresponding DIN-Tests.

Sample Name	PLA Grade	Grammage	Fiber Fineness	Thickness	Air Permeability
NW-I	Ingeo™ 6100D + 7% PBS	114 gsm	1.9 dtex	0.72 mm	1643 l/qm/s
NW-L	Luminy® L130	123 gsm	5.1 dtex	0.90 mm	2606 l/qm/s

2.4. Artificial Aging Procedure

The artificial aging of the samples was performed in a climatic chamber WK1-340 (Weiss Umwelttechnik GmbH, Oberhausen, Germany) without additional fixation of the fibers or fabrics. The conditions were varied in the range of 20–95% of the relative humidity (RH) and 50–70 °C. Aging period was two weeks for monofilaments and seven days for nonwovens. The treated samples were stored under ambient conditions prior to characterization of their thermal and mechanical behavior.

2.5. Mechanical Testing

All presented tensile tests were carried out using a universal testing machine EZ 50 and a 1 kN load cell (Zwick/Roell GmbH, Haan, Germany) after 24 h of air conditioning at RT (T = 23 °C; RH = 50%). Five repeated measurements were taken for each reported sample. In accordance with DIN EN 13895/DIN EN ISO 13934, the strain rates are 250 and 100 mm/min with clamping lengths of 250 and 100 mm, respectively. For tensile tests 50 cm-long monofilaments and 30 × 5 cm²-large nonwoven sheets were used

2.6. Filtration Tests

Filtration tests were performed on a 11.3 cm-wide PLA nonwoven NW-L before and after artificial aging using a standard test bench at Institut für Energie- und Umwelttechnik (IUTA, Duisburg, Germany) under the following parameters: flow velocity 15.0 cm/s, T = 20 °C and RH = 50%. KCl particles were produced using aerosol generator AGK-2000 (Palas GmbH, Karlsruhe, Germany) under a volume flow of 90 L/min and an input pressure of 0.8 bar.

2.7. Fourier Transform Infrared Spectroscopy (FTIR)

FTIR measurements were taken with an IRPrestige-21 Spectrophotometer in combination with the Golden-Gate Diamond ATR Unit (Shimadzu, Kyoto, Japan) using the software LabSolutions IR. Monofilaments and fabrics were measured both in solid state and for comparison as a thick film casted from 2–5 w% chloroform solutions of the respective materials. Sapphire press plunger was used to measure solid samples and casted films, while a concave press plunger was used in case of highly degraded (pulverized) samples.

2.8. Differential Scanning Calorimetry (DSC)

DSC measurements were conducted on samples with a weight of 4–5 mg using a Q20 instrument (TA Instruments, New Castle, DE, USA) under nitrogen atmosphere and cooling with compressed air. A standard heating rate of 10 °C/min was applied for the first heating run (and also for the second run) followed by cooling down to the starting temperature of 40 °C with a maximum cooling rate and a 10 min isothermal before the second heating.

2.9. Scanning Electron Microscopy (SEM)

Fiber morphology was studied by scanning electron microscopy (Hitachi S-3400 Type II, Hitachi High-Technologies Europe GmbH, Krefeld, Germany).

2.10. 3D Optical Microscopy

The microscopic images of the monofilament and nonwoven materials were taken with a VHX digital microscope from Keyence Deutschland GmbH (Neu-Isenburg, Germany).

2.11. Gel Permeation Chromatography (GPC)

A device by Shimadzu Deutschland GmbH (Duisburg, Germany) with a column-set consisting of one precolumn (SDV 5 μm 8 \times 50 mm (PSS GmbH, Mainz, Germany) and two separation columns (SDV 1000 \AA 5 μm 8 \times 300 mm and SDV 100.000 \AA 5 μm 8 \times 300 mm, PSS GmbH, Mainz, Germany) was used for the measurements of the average molecular weight of PLA before and after treatment for selected samples. PLA fibers were dissolved in chloroform (HPLC grade) to achieve a nominal concentration of 2.5 mL/mg. Chloroform was used as an eluent at a flow rate of 1 mL/min. Poly(methyl methacrylate) standards were used for the calibration.

3. Results and Discussion

3.1. Approach for Elaboration of Degradation Behavior of PLA Monofilaments

Degradation of tough PLA monofilaments under elevated temperature and humidity conditions has been reported earlier [29]. In that study, a combination of physical and chemical methods, including DSC measurements, molar mass determination, tensile tests and relaxation measurements were employed to assess initial stages of mechanical failure of the fibers as a result of hydrolytic degradation (Figure 1). This combination has proven to be suitable for indicating small changes in material properties, which allowed us to define monofilaments as stable or showing signs of degradation, implying that the initial material properties may no longer satisfy the targeted application. Figure 1a presents the stress–strain curves of PLA monofilaments aged at 60 °C, which reveal a typical behavior of elastic polymer fibers with high strength and good ductility, i.e., relatively high elongation before break. As can be seen, however, gradual changes in the mechanical performance develop with the increase in the humidity, suggesting an effect of water molecules on plasticizing and on the rate of hydrolysis [20,44,45]. It is important to note that elastic properties, i.e., modulus and yield strength, are only affected at a humidity in excess of 65%. Although the samples treated at high humidity still maintain good mechanical integrity and strength, they are assigned to degraded states (Figure 1b). The hydrolytic degradation state was confirmed by chemical analysis (GPC), which revealed a reduction in the molecular weight (Figure 2). We note that monofilaments which were treated at high humidity and elevated temperature conditions (close to T_g) are characterized by extreme brittleness and by a complete loss of mechanical integrity (Figure 1c,d). In contrast, monofilaments stored at room conditions for almost 20 months exhibited mechanical and relaxation properties very close to that measured shortly after their fabrication.

Good storage properties at mild environmental conditions of PLA fibers studied here underline important advantages of industrial fabrication as compared to laboratory scale devices. Reported PLA films, tubes [46,47] or injected/extruded samples [48], produced under laboratory conditions, exhibit elastic moduli and strengths generally below 4 GPa and 40–70 MPa, respectively, and strains below 10%. In such samples, even after improving the crystallinity degree by large-scale plastic deformation or by thermal annealing, the fraction of the amorphous phase still comprises 40–50%, so that the material can turn brittle rapidly as a result of physical aging; in some reported cases, this occurred after several hours of storage at room temperature [20,49].

We note that, while thermal properties and molecular weight distribution indicate measurable changes in the samples, which show advanced degradation behaviors, the relaxation measurement, evaluated via a lifetime prediction model, has been proven to be the most sensitive in revealing changes, which leads to a slight improvement of the mechanical performance. This knowledge allows one to use defined environmental conditions in order to self-reinforce the highly crystalline and oriented structure allotted by the fabrication [29].

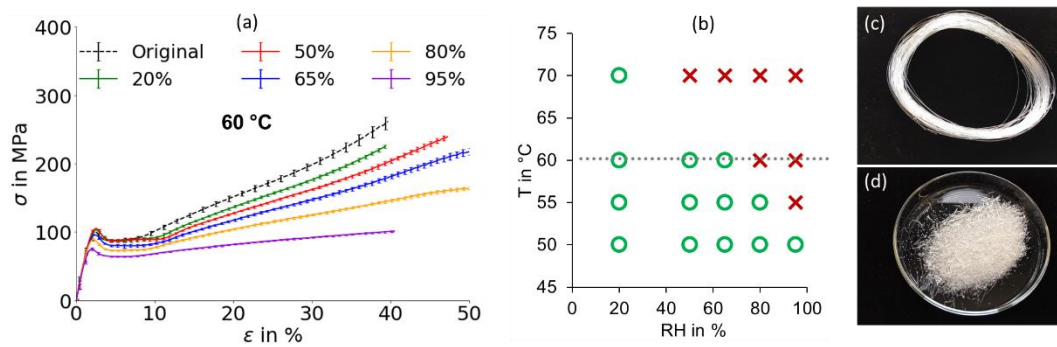


Figure 1. (a) Stress–strain curves of monofilaments subjected to artificial aging at 60 °C and indicated relative humidity (%) for two weeks. (b) Diagram of stability in terms of RH and aging temperature showing conditions which correspond to mechanically stable (green circles) and mechanically weakened/degraded (red crosses) samples after two weeks of treatment. The dashed line indicates the samples displayed in (a). (c,d) Images of mechanically intact and completely degraded monofilaments, respectively. The latter was treated under 70 °C and 95% RH for two weeks. Reprinted with adoptions from Ref [29].

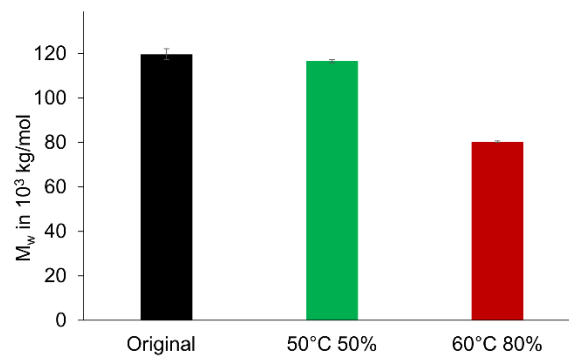


Figure 2. Molecular weight, determined with GPC, of PLA in fibers after manufacturing (original) and after artificial aging under indicated conditions.

Relaxation tests, however, are not feasible for fibrous textile materials due to the high degree of their inhomogeneity related to fiber distribution and to the fabric density. Moreover, the mechanical strength of a nonwoven fabric is defined rather by the strength provided by the bonding step, rather than by the mechanical strength of single fibers. Therefore, in-depth characterization of the degradation or self-reinforcement behavior of PLA-based nonwovens requires partially different approaches as compared to single monofilaments. In the following, we analyze the ability of conventionally used and modified methodologies to predict the durability of PLA nonwovens, particularly under elevated temperature and humidity conditions.

3.2. Thermal Analysis of PLA-Based Materials

Differential scanning calorimetry is widely used to assess the physical aging of PLA by evaluating the changes in T_g and enthalpy recovery associated with the chain relaxations [15].

Puchalski et al. [27] used DSC along with other methods of structural and chemical analysis for the evaluation of molecular ordering and creation of meso and crystalline structures of PLA during the fabrication of spun-bonded nonwoven in the downstream pilot laboratory equipment. The increase in take-up velocity and calendaring temperatures well above T_g leads to formation of about 60% of ordered crystalline phase. However, it should be noted that an additional reduction in the initial molecular weight can occur during high-temperature processing as a result of the thermal degradation of PLA, reaching as much as 60% [40,50]. This effect is illustrated in Figure 3a,b which compares DSC curves of the original pellet material, monofilament and nonwoven fabric.

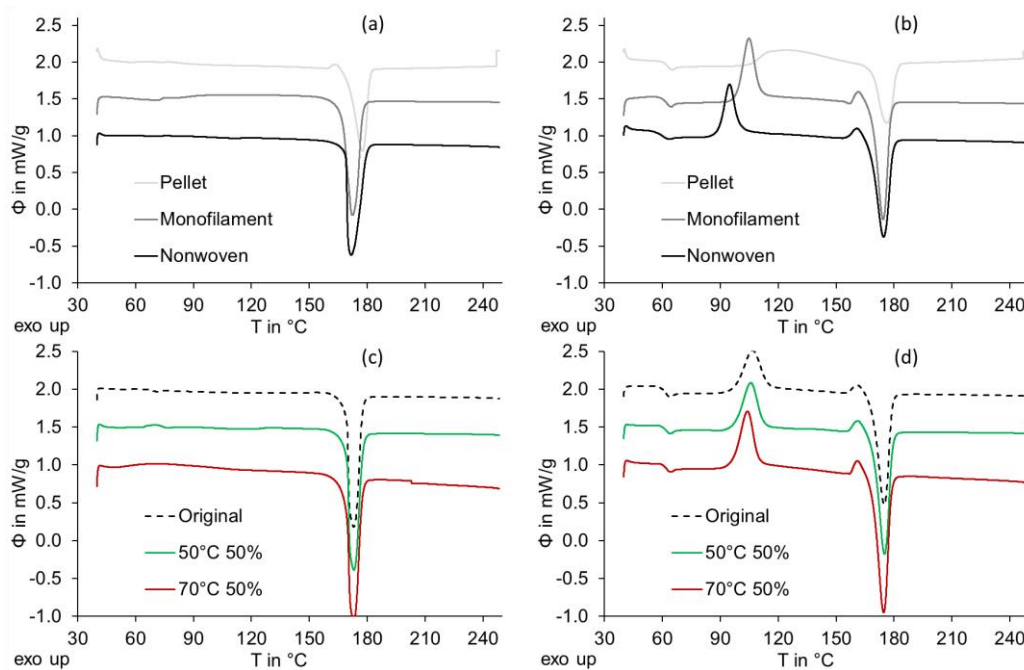


Figure 3. DSC thermograms, first (a,c) and second (b,d) runs, of PLA materials: (a,b) pellet, monofilament and nonwoven NW-I of the same grade PLA; (c,d) nonwoven NW-L before and after artificial aging under indicated conditions.

As can be seen in first DSC heating run (Figure 3a), all samples are semi-crystalline with a missing cold crystallization peak. The degree of crystallinity, calculated as described in [29], using an ideal melting enthalpy of $\Delta H_m^0 = 93.7 \text{ J/g}$, is $\sim 72\%$ for pellets, $\sim 75\%$ for nonwovens and slightly higher ($\sim 78\%$) for the monofilaments. The crystallinity has a high impact on the resulting mechanical properties of the fibers, i.e., on the elasticity and tensile strength. On the other hand, crystallization is influenced by the molecular weight (chain length) and the chain orientation during processing. The second run curves in Figure 3b clearly reveal differences in the shape and the position of the melting peak for thermally processed PLA from the original pellet material. The decrease in 2°C of T_m can be clearly attributed to a partial thermal degradation as a result of high-temperature processing. Furthermore, a broad cold crystallization peak at $\sim 120^\circ\text{C}$ for pellets is significantly shifted for fabricated materials, indicating a lower amount of energy required for crystallization of shorter and oriented chains. Note that cold crystallization process appears different for extruded monofilaments and nonwovens, indicating influence of the processing on the resulting materials properties.

DSC curves of nonwovens treated at indicated conditions (Figure 3c,d) can be assessed along the same lines. The first run curves reveal minor changes after the treatment of the nonwovens. The degree of crystallinity ($\sim 73\%$ for the original sample) slightly increases in the case of the treatment at 70°C and $50\% \text{ RH}$ (degree of crystallinity $\sim 78\%$) and 70°C and $50\% \text{ RH}$ (degree of crystallinity $\sim 81\%$). Together with a slight decrease in T_m and T_c temperatures for this sample in the second run (Figure 3d), the results might indicate a partial chain scission as a result of hydrolysis. It is, however, natural that above T_g the enhanced chain mobility facilitates the diffusion of water. Additionally, the rate constant of hydrolysis increases as the temperature grows [20–22].

3.3. Mechanical Tests of Artificially Aged Nonwovens

In order to correlate the DSC results with the mechanical integrity of the nonwovens, tensile tests were performed. An essential task of this study is the assessment of a principal suitability of the tensile tests on nonwoven materials to evaluate the initial steps of the aging behavior. The intrinsic inhomogeneity in nonwovens fabrics is known to be as large as 20% , while the sought structural and mechanical changes might be hidden in

the intrinsic scatter between different fabric pieces. To assess the range of accuracy and reproducibility of the measurements, nonwoven sheets were measured lengthwise and crosswise, with the direction of the fabric predefined by the transport direction of the belt during the fabrication.

Figure 4 illustrates a clear difference in the mechanical performance depending on the processing parameters, direction of the textile with randomly oriented fibers (Figure 4b,d), as well as the range of the scatter. In the following, the treated and untreated fabrics were tested “lengthwise”. It is anticipated that the degradation of PLA will affect both the entanglements between the fibers and the mechanical strength of individual fibers.

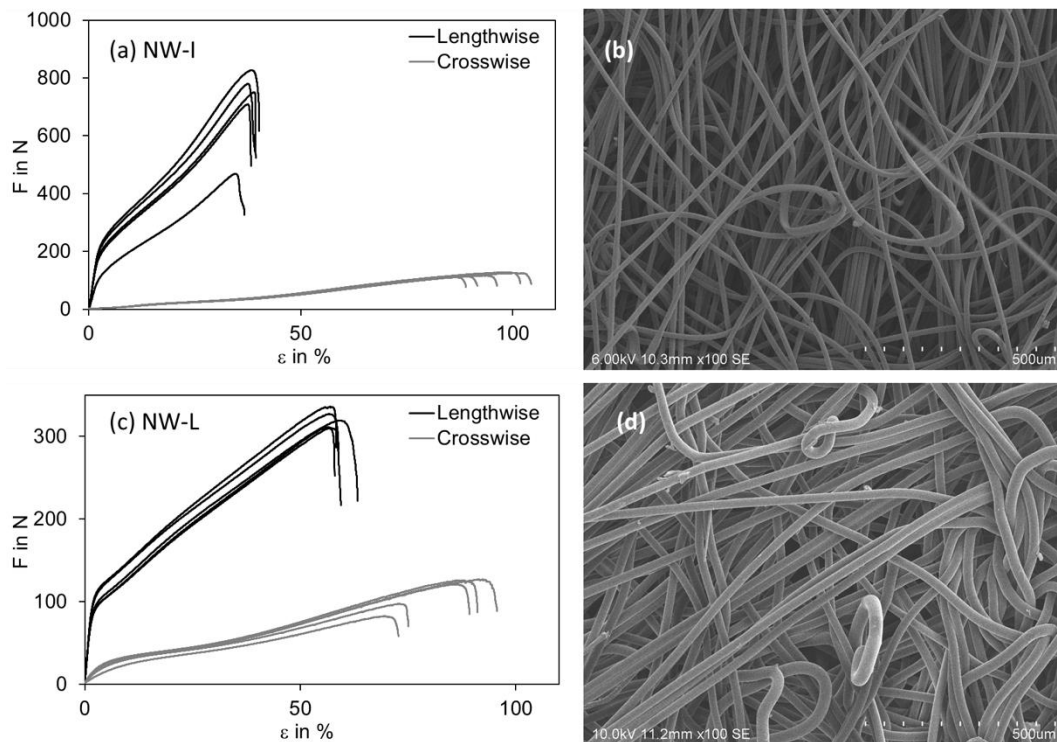


Figure 4. (a,c) Force–strain curves measured on NW-I and NW-L fabrics, respectively, along lengthwise and crosswise directions. SEM images of the nonwovens (b) NW-I and (d) NW-L.

Shown in Figure 5 is the stability diagram of nonwoven NW-L, which was artificially aged for 7 days instead of two weeks for monofilaments (Figure 1b). The evaluation was based on the assessment of the deviations of the tensile–stress curves of the treated samples from that of the original nonwoven (shown in Figure 5b–d).

It can be seen that the deviation both in elastic range (up to 2% strain ϵ) and in the plastic deformation before break is relatively large, though clear trends can be identified: increasing the temperature (Figure 5b,c) and humidity (Figure 5d) of the aging condition leads to a decrease in the strength and in the elongation at break. We note that the boundary of stable conditions for monofilaments in Figure 1b and nonwovens only apparently look similar, since the latter have been subjected to aging for a significantly shorter time. A faster degradation of nonwovens is attributed to much fine fiber diameters and, most importantly, to the differences in the performed melt extrusion processing. Further detailed investigations, including structural analysis, are in progress.

Exposure to extreme aging conditions of 80 °C and 80% RH leads to an extreme brittleness of the fabrics, so that the samples are not possible to handle. Figure 6a,b present optical images of the loose fabric, as well as REM images of the fibers after (Figure 6c) and before aging (Figure 6d). The latter sample reveals numerous broken fibers even on a small-sized area of the nonwoven.

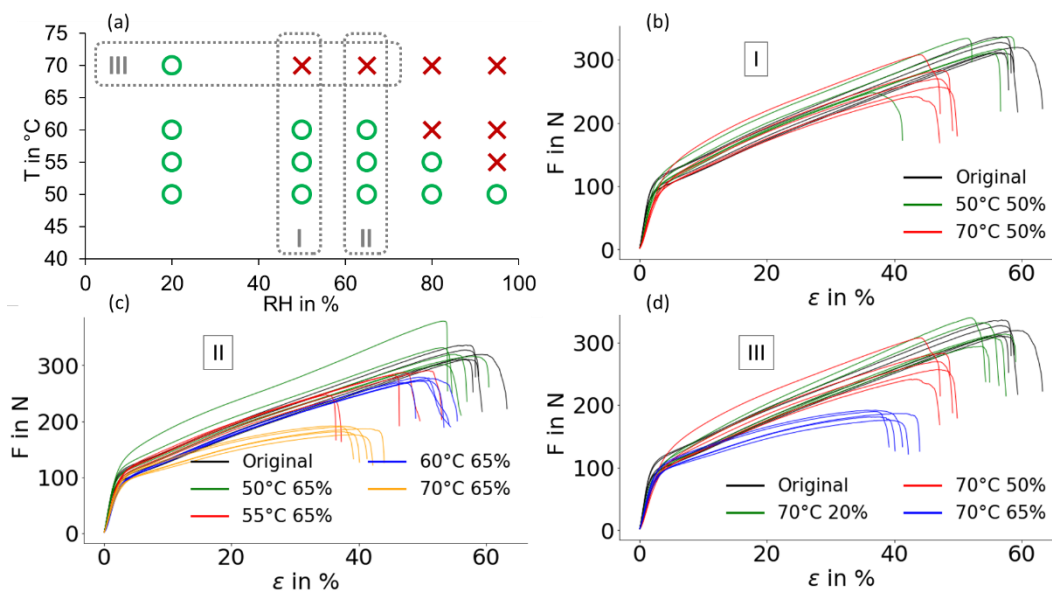


Figure 5. (a) Diagram of the apparent stability of nonwoven NW-L in terms of RH and aging temperature (showing conditions which correspond to mechanically stable (green circles) and mechanically weakened/degraded (red crosses) samples after 7 days of treatment). (b–d) Exemplary stress–strain curves of artificially aged nonwovens at indicated conditions, which are grouped in (I–III), as indicated by respective rectangles in the diagram.

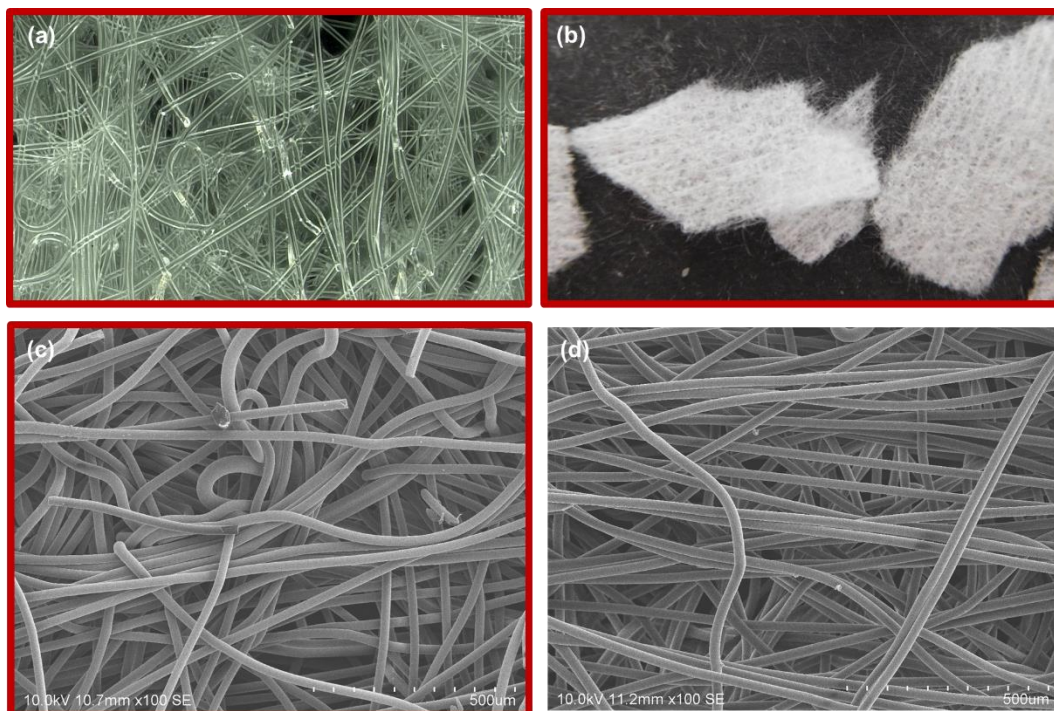


Figure 6. (a) 3D optical microscopy, (b) macroscopic photo of the fabric NW-L pieces treated at 80 °C and 80% RH for 7 days. (c,d) SEM images of the fibers after and before the aging, respectively, with the aged sample revealing numerous broken ends.

We note that assignment to the sample treated, e.g., at 70 °C/50% RH a degradation behavior was based on the results of destructive analysis, such as DSC (Figure 3d) and tensile tests (Figure 5b), although the nonwoven fabric remained mechanically intact and thus showed only initial stages of the mechanical failure as a result of hydrolytic degradation. In the following, we assess the limits of FTIR spectroscopy to identify the

onset of chemical and structural changes which accompany hydrolytic degradation of PLA highly crystalline fibrous materials.

3.4. Characterization Using FTIR Spectroscopy

FTIR spectroscopy is a fast and noninvasive method which has been intensively used for the analysis of hydrolytically degraded PLA materials, as well as for the evaluation of the changes in the crystalline and amorphous states in the course of physical aging, annealing or under influence of processing [36,38,44,51–57]. The measured FTIR spectra are presented in Figure 7.

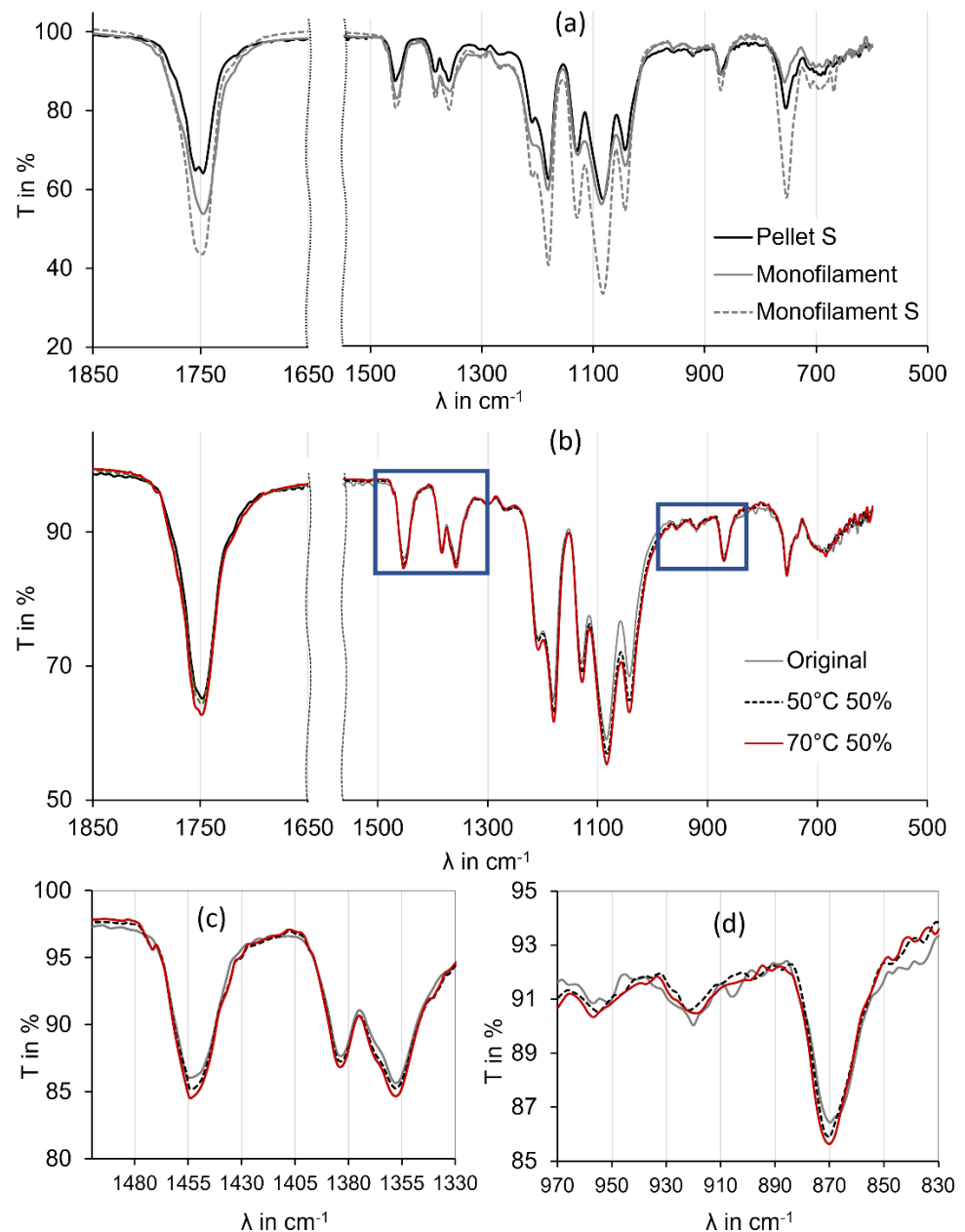


Figure 7. FTIR spectra of PLA materials: (a) monofilament as fabricated and cast from solution (S) and cast film of pellet material of the same grade; (b–d) as prepared (original) and artificially aged nonwoven NW-L under indicated conditions. Rectangles in (b) mark the enlarged areas of spectra displayed in (c,d).

Lactic acid peaks of the backbone are located at 1150 and 998 cm^{-1} , while polymeric PLA shows more peaks, shifted to other wavenumbers due to conjugations at about 1119, 1040 and 1207 cm^{-1} and should be visible upon degradation [38]. Lactic acid and its oligomers terminated by hydroxyl and carboxyl end groups are typically identified as hydrolytic degradation products as a result of random scission of the ester bonds. Braun et al. [51] have rationalized the lactide ring breathing mode peak at 935 cm^{-1} against the asymmetric bending mode of methyl groups at 1454 cm^{-1} . Since a methyl group is present both in the lactide monomer and the polymer, this ratio is envisaged to provide a direct measure of lactide conversion [53].

Additionally, hydrolysis- or processing-induced molecular ordering and evolution of a stable α -crystal form into instable α' -form of PLA can be deduced from the FTIR spectra, with α' -phase crystallites forming at relatively high temperature and humidity [27,52,58]. Generally, the carboxyl stretching region (1700–1800 cm^{-1}) and ester groups vibrational modes between 1300 and 1000 cm^{-1} are known to be sensitive to the conformation of the chain, and therefore can be used to differentiate the crystalline forms of PLA. Chen et al. [52] reported that the α -phase leads to band splitting at 1750 cm^{-1} , while the α' -form only shows one band, and that α' crystallites formed during hydrolytic degradation rather than the α -phase. However, other interpretations of the band splitting at 1750 cm^{-1} exist [54,58], referring to the presence of monomeric units in the matrix of carboxylic acids bound by esters and thus indicating a degradation process. This would explain the formation of a second peak at 1760 cm^{-1} representing the monomeric unit. Additionally, the bands at ~921 and 957 cm^{-1} are assigned to the nonspecific crystalline phase (or mesophase) and to the amorphous phase, respectively. At the same time, the shape of the FTIR spectra and, accordingly, the interpretation of the related structural and chemical changes in PLA samples differs from study to study.

In order to facilitate the evaluation of the sought effects, we first performed FTIR measurements on highly oriented and highly crystalline PLA monofilaments and compared them with the spectra measured on films casted from chloroform solution of the monofilaments as well as from the solutions of raw pellet PLA material (Figure 7a). The expectations behind were to separate the orientation of the crystalline phase (solid and casted monofilament materials) and strong decrease in molar mass (casted pellets and monofilament), both effects being imposed by the fabrication process.

As can be seen in Figure 7a, the spectra of three samples differ in all main bands, which are identified for PLA. A higher degree of crystallinity can be assigned to casted monofilament due to the highest intensity of peaks at 1750 and 757 cm^{-1} . At the same time, the pronounced intensities at 1454 and 871 cm^{-1} bands, corresponding, respectively, to vibrations of methyl groups and the amorphous state, likely indicate the decrease in the molecular weight as compared to the raw pellet material. The most pronounced differences are seen in the region linked to ester groups between 1300 and 1000 cm^{-1} , which should be sensitive to conformational changes of the α' and α forms of PLA. However these bands exhibit a strong tendency of overlap, making the analysis and interpretation less feasible [56].

Figure 7b compares the spectra of nonwovens before and after artificial aging at mild and elevated temperatures. The close up areas of the most relevant areas of spectra (Figure 7c,d) reveal a weak trend of the degree of crystallinity increasing as the temperature of aging grows. The shape of the peak at 1750 cm^{-1} is not notably affected as a result of aging. Additionally, the bands at 921 and 957 cm^{-1} appear to be similar, indicating no significant structural changes.

3.5. Probing the Degradation Stability of Nonwovens in Filtration Tests

The relaxation tests combined with a lifetime prediction model have proven to be the most sensitive when assessing the chemical and structural changes in artificially aged monofilaments [29]. However, this type of measurement is principally not suitable for fibrous fabrics. Therefore, in order to gain deeper insights into the hydrolysis resistance

of PLA nonwovens, filtration tests were used for comparison of in situ and ex situ aged nonwoven fabrics. Along with the changes in the mechanical integrity, filtration tests provide indirect evidence on the surface properties of individual fibers, which is reflected in the separation efficiency of the tested filter media.

Figure 8 presents the separation efficiency of the untreated and of artificially aged nonwovens (as in Figure 5). Although the nonwoven architecture used was not optimized for use as a filter material, a good separation efficiency η is achieved for particles with dimensions above 3 μm . The sample, which was artificially aged prior to filter tests under mild conditions (50 °C, 50% RH), exhibited no reduction in the filter performance in comparison to the untreated sample (original). The sample aged at extreme conditions (70 °C, 50% RH) had a significantly lower filter performance in the whole studied range but shows no increase in the air pressure difference (~24 Pa for all three samples). This observation could, on the one hand, indicate a fast decrease in mechanical integrity as soon as the media are increasingly loaded with the particles and the pressure on individual fibers grows. We note that the visualization of fiber morphology in SEM images (Figure 7b,c) does not reveal appearance of broken fibers. On the other hand, the separation efficiency in sub-micrometer range depends on the surface properties of the fibers. Therefore, additional tests are required to characterize a possible loss in the surface hydrophobicity or in electret function. Generally, the results of the filtration tests are in good agreement with the stability diagram in Figure 5.

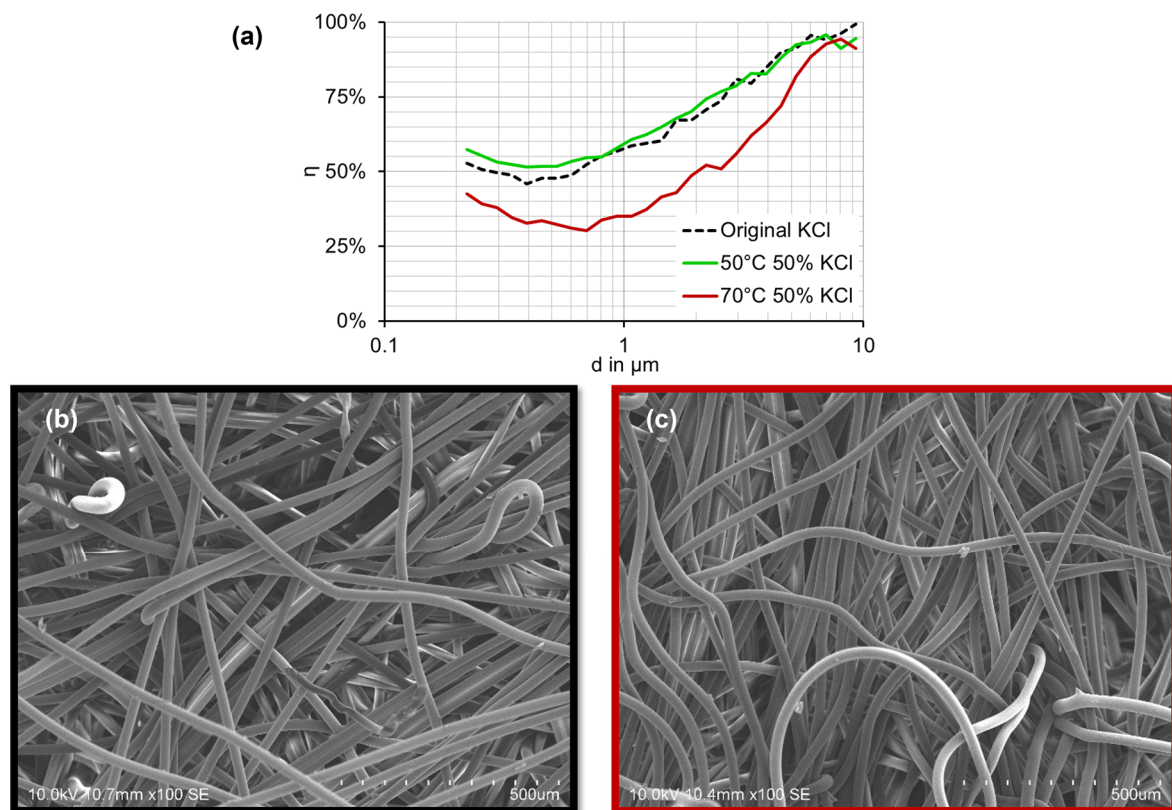


Figure 8. (a) Separation efficiency η of PLA nonwoven NW-L tested using generated KCL particles before (original) and after artificial aging at indicated conditions. (b,c) SEM images of original nonwoven and nonwoven after aging at 70 °C and 50% RH.

4. Conclusions

The presented work suggests approaches to solve the challenge of evaluating the life and service time of degradable nonwovens under particular application conditions. In contrast to extruded or injection molded samples, the mechanical property of fibrous

materials cannot be straightforwardly characterized by tensile moduli or tensile stress, especially when the material is prone both to physical aging and to chemical degradation. Additionally, the relaxation tests are not feasible to perform on nonwoven fabrics.

Industrially melt-spun PLA monofilaments and nonwovens have been subjected to environmental aging for up to 14 days at a temperature range of 50–70 °C, below and above the glass transition temperature of the material, and at 20–95% relative humidity. The effect of the hydrolytic degradation on the mechanical performance of highly crystalline fibers has been assessed by analyzing their thermal and mechanical properties. The data indicate that treatments at high humidity and elevated temperature expectedly lead to a weakening of the PLA materials. On the other hand, a durable performance is preserved after storage under moderate weathering conditions (e.g., 50 °C 50% RH). The diagrams of stability and hydrolytic degradation are presented for both types of PLA materials which have been aged for 7–14 days in a wide range of temperatures and humidity.

Special focus has been given to the assessment of the initial stages of the degradation, when materials maintained their mechanical integrity. DSC, FTIR and tensile tests all demonstrate a moderate sensitivity and informativity in assessment of the small changes in the crystalline structure and in chemical composition.

Further, the results of the filtrations tests on already aged nonwovens conformed with the boundaries of hydrolytic resistivity in the stability diagram. These promising results confirm the potential of PLA-nonwoven media in air filtration under moderate climatic conditions—up to max 50 °C, 50% RH—with currently available PLA grades and manufacturing process. On the other hand, for each targeted application, a specific aging procedure has to be developed, which possibly models all external effects. In case of potential application in air filtration, and additionally possibly in temperature and humidity variations, a permanent (or periodic) pressure flow is exerted on the material, which can change the degradation mechanisms and dynamics. Standard tests to specify fibrous materials with biodegradable components including lifetime assessment still have to be elaborated.

Author Contributions: Conceptualization, L.T. and R.T.; methodology, C.S. and E.M.; validation, C.S. and L.T.; investigation, C.S. and L.T.; resources, J.S.G. and R.T.; writing—original draft preparation, C.S.; writing—L.T. and C.S.; supervision, L.T. and J.S.G.; project administration, L.T. and R.T.; funding acquisition, J.S.G., L.T. and R.T. All authors have read and agreed to the published version of the manuscript.

Funding: The research project IGF-Nr. 19812 BG is funded by the German Federation of Industrial Research Associations (AiF) within the program for sponsorship by Industrial Joint Research (IGF) of the German Federal Ministry of Economic Affairs and Energy based on an enactment of the German Parliament.

Institutional Review Board Statement: Not applicable.

Informed Consent Statement: Not applicable.

Data Availability Statement: Data sharing not applicable.

Acknowledgments: The authors thank Michael Luksin (Hochschule Hamm-Lippstadt, University of Applied Sciences, Germany) for the GPC measurements. K. Schulte and N. Fischer (Monofil-Technik GmbH, Germany) are acknowledged for the fabrication of the monofilaments and K. Knopf and E. Cleve (Hochschule Niederrhein, University of Applied Sciences, Germany) are acknowledged for providing the equipment for the mechanical tests.

Conflicts of Interest: The authors declare no conflict of interest.

References

1. Lim, L.-T.; Auras, R.; Rubino, M. Processing technologies for poly(lactic acid). *Prog. Polym. Sci.* **2008**, *33*, 820–852. [[CrossRef](#)]
2. Vink, E.T.H.; Rábago, K.R.; Glassner, D.A.; Springs, B.; O'Connor, R.P.; Kolstad, J.; Gruber, P.R. The sustainability of NatureWorks polylactide polymers and Ingeo polylactide fibers: An update of the future. *Macromol. Biosci.* **2004**, *4*, 551–564. [[CrossRef](#)] [[PubMed](#)]

3. Vadas, D.; Kmetykó, D.; Marosi, G.; Bocz, K. Application of Melt-Blown Poly(lactic acid) Fibres in Self-Reinforced Composites. *Polymers* **2018**, *10*, 766. [[CrossRef](#)]
4. Gupta, B.; Revagade, N.; Hilborn, J. Poly(lactic acid) fiber: An overview. *Prog. Polym. Sci.* **2007**, *32*, 455–482. [[CrossRef](#)]
5. Mallegni, N.; Phuong, T.V.; Coltelli, M.-B.; Cinelli, P.; Lazzeri, A. Poly(lactic acid) (PLA) Based Tear Resistant and Biodegradable Flexible Films by Blown Film Extrusion. *Materials* **2018**, *11*, 148. [[CrossRef](#)] [[PubMed](#)]
6. Raghvendra, K.M.; Sravanthi, L. Fabrication Techniques of Micro/Nano Fibres based Nonwoven Composites: A Review. *Mod. Chem. Appl.* **2017**, *5*, 1000206. [[CrossRef](#)]
7. Gazzola, W.H.; Benson, R.S.; Carver, W. Meltblown Poly(lactic acid) Nanowebs as a Tissue Engineering Scaffold. *Ann. Plast. Surg.* **2019**, *83*, 716–721. [[CrossRef](#)]
8. Liu, J.; Zhang, X.; Zhang, H.; Zheng, L.; Huang, C.; Wu, H.; Wang, R.; Jin, X. Low resistance bicomponent spunbond materials for fresh air filtration with ultra-high dust holding capacity. *RSC Adv.* **2017**, *7*, 43879–43887. [[CrossRef](#)]
9. Jafari, M.; Shim, E.; Joojode, A. Fabrication of Poly(lactic acid) filter media via the meltblowing process and their filtration performances: A comparative study with polypropylene meltblown. *Sep. Purif. Technol.* **2021**, *260*, 118185. [[CrossRef](#)]
10. Bahners, T.; Tsarkova, L.; Gebert, B.; Gutmann, J.S. Functionalization of textiles by deposition of UV-cured organic thin layers with charge storage properties for electronic and environmental technology. *Prog. Org. Coat.* **2021**, *157*, 106332. [[CrossRef](#)]
11. Slack, R.W. New structures for resorbable polymers. *Chem. Fibers Int.* **2010**, *60*, 236–237.
12. Fambri, L.; Migliaresi, C. Crystallization and Thermal Properties. In *Poly(Lactic Acid)*; Auras, R., Lim, L.-T., Selke, S.E.M., Tsuji, H., Eds.; John Wiley & Sons, Inc.: Hoboken, NJ, USA, 2010; Volume 1, pp. 113–124.
13. Laycock, B.; Nikolić, M.; Colwell, J.M.; Gauthier, E.; Halley, P.; Bottle, S.; George, G. Lifetime prediction of biodegradable polymers. *Prog. Polym. Sci.* **2017**, *71*, 144–189. [[CrossRef](#)]
14. Schippers, C.; Cleve, E.; Bahners, T.; Gutmann, J.S.; Tsarkova, L. Improved Maxwell Model Approach and its Applicability towards Lifetime Prediction of Biobased Viscoelastic Fibers. *Macromol. Mater. Eng.* **2021**. [[CrossRef](#)]
15. Cui, L.; Imre, B.; Tatraaljai, D.; Pukanszky, B. Physical ageing of poly(lactic acid): Factors and consequences for practice. *Polymer* **2020**, *186*, 122014. [[CrossRef](#)]
16. Li, K.; Wang, Y.; Rowe, M.; Zhao, X.; Li, T.; Tekinalp, H.; Ozcan, S. Poly(lactic acid) Toughening through Chain End Engineering. *ACS Appl. Polym. Mater.* **2020**, *2*, 411–417. [[CrossRef](#)]
17. Monnier, X.; Delpouve, N.; Saiter-Fourcin, A. Distinct dynamics of structural relaxation in the amorphous phase of poly(L-lactic acid) revealed by quiescent crystallization. *Soft Matter* **2020**, *16*, 3224–3233. [[CrossRef](#)] [[PubMed](#)]
18. Simmons, H.; Tiwary, P.; Colwell, J.E.; Kontopoulou, M. Improvements in the crystallinity and mechanical properties of PLA by nucleation and annealing. *Polym. Degrad. Stab.* **2019**, *166*, 248–257. [[CrossRef](#)]
19. Liu, G.; Zhang, X.; Wang, D. Tailoring crystallization: Towards high-performance poly(lactic acid). *Adv. Mater.* **2014**, *26*, 6905–6911. [[CrossRef](#)]
20. Rocca-Smith, J.R.; Whyte, O.; Brachais, C.-H.; Champion, D.; Piasente, F.; Marcuzzo, E.; Sensidoni, A.; Debeaufort, F.; Karbowski, T. Beyond Biodegradability of Poly(lactic acid): Physical and Chemical Stability in Humid Environments. *ACS Sustain. Chem. Eng.* **2017**, *5*, 2751–2762. [[CrossRef](#)]
21. Mitchell, M.K.; Hirt, D.E. Degradation of PLA fibers at elevated temperature and humidity. *Polym. Eng. Sci.* **2015**, *55*, 1652–1660. [[CrossRef](#)]
22. Gorrasi, G.; Pantani, R. Hydrolysis and Biodegradation of Poly(lactic acid). In *Synthesis, Structure and Properties of Poly(lactic acid)*; Di Lorenzo, M.L., Androsch, R., Eds.; Springer International Publishing: Cham, Switzerland, 2018. [[CrossRef](#)]
23. Shi, B.; Palfery, D. Enhanced Mineralization of PLA Meltblown Materials Due to Plasticization. *J. Polym. Environ.* **2010**, *18*, 122–127. [[CrossRef](#)]
24. Gieldowska, M.; Puchalski, M.; Szparaga, G.; Krucińska, I. Investigation of the Influence of PLA Molecular and Supramolecular Structure on the Kinetics of Thermal-Supported Hydrolytic Degradation of Wet Spinning Fibres. *Materials* **2020**, *13*, 2111. [[CrossRef](#)]
25. Dharmalingam, S.; Hayes, D.G.; Wadsworth, L.C.; Dunlap, R.N. Analysis of the time course of degradation for fully biobased nonwoven agricultural mulches in compost-enriched soil. *Text. Res. J.* **2016**, *86*, 1343–1355. [[CrossRef](#)]
26. Hammonds, R.L.; Gazzola, W.H.; Benson, R.S. Physical and thermal characterization of poly(lactic acid) meltblown nonwovens. *J. Appl. Polym. Sci.* **2014**, *131*. [[CrossRef](#)]
27. Puchalski, M.; Sulak, K.; Chrzanowski, M.; Sztajnowski, S.; Krucińska, I. Effect of processing variables on the thermal and physical properties of poly(L-lactide) spun bond fabrics. *Text. Res. J.* **2014**, *85*, 535–547. [[CrossRef](#)]
28. Liu, Q.; Sun, Y.; Xia, S.; Zhang, H.; Tao, X.; Liu, Y.; Deng, B. Structure and mechanical property of polylactide fibers manufactured by air drawing. *Text. Res. J.* **2016**, *86*, 948–959. [[CrossRef](#)]
29. Schippers, C.; Bahners, T.; Gutmann, J.S.; Tsarkova, L.A. Elaborating Mechanisms behind the Durability of Tough Polylactide Monofilaments under Elevated Temperature and Humidity Conditions. *ACS Appl. Polym. Mater.* **2021**, *3*, 1406–1414. [[CrossRef](#)]
30. Zaaba, N.F.; Jaafar, M. A review on degradation mechanisms of poly(lactic acid): Hydrolytic, photodegradative, microbial, and enzymatic degradation. *Polym. Eng. Sci.* **2020**, *60*, 2061–2075. [[CrossRef](#)]
31. Woodard, L.N.; Grunlan, M.A. Hydrolytic Degradation and Erosion of Polyester Biomaterials. *ACS Macro Lett.* **2018**, *7*, 976–982. [[CrossRef](#)]

32. Höglund, A.; Odellius, K.; Albertsson, A.-C. Crucial Differences in the Hydrolytic Degradation between Industrial Polylactide and Laboratory-Scale Poly(L-lactide). *ACS Appl. Mater. Interfaces* **2012**, *4*, 2788–2793. [[CrossRef](#)]
33. Liu, Y.; Cheng, B.; Cheng, G. Development and filtration performance of polylactic acid meltblowns. *Text. Res. J.* **2010**, *80*, 771–779. [[CrossRef](#)]
34. Zhang, J.; Chen, G.; Bhat, G.S.; Azari, H.; Pen, H. Electret characteristics of melt-blown polylactic acid fabrics for air filtration application. *J. Appl. Polym. Sci.* **2020**, *137*, 48309. [[CrossRef](#)]
35. Bergstrom, J.S.; Hayman, D. An Overview of Mechanical Properties and Material Modeling of Polylactide (PLA) for Medical Applications. *Ann. Biomed. Eng.* **2016**, *44*, 330–340. [[CrossRef](#)]
36. Porfyrus, A.; Vasilakos, S.; Zotiadias, C.; Papaspyrides, C.; Moser, K.; van der Schueren, L.; Buyle, G.; Pavlidou, S.; Vouyiouka, S. Accelerated ageing and hydrolytic stabilization of poly(lactic acid) (PLA) under humidity and temperature conditioning. *Polym. Test.* **2018**, *68*, 315–332. [[CrossRef](#)]
37. Razavi, M.; Wang, S.-Q. Why Is Crystalline Poly(lactic acid) Brittle at Room Temperature? *Macromolecules* **2019**, *52*, 5429–5441. [[CrossRef](#)]
38. Jariyasakoolroj, P.; Tashiro, K.; Wang, H.; Yamamoto, H.; Chinsirikul, W.; Kerddonfag, N.; Chirachanchai, S. Isotropically small crystalline lamellae induced by high biaxial-stretching rate as a key microstructure for super-tough polylactide film. *Polymer* **2015**, *68*, 234–245. [[CrossRef](#)]
39. Li, C.; Jiang, T.; Wang, J.; Wu, H.; Guo, S.; Zhang, X.; Li, J.; Shen, J.; Chen, R.; Xiong, Y. In Situ Formation of Microfibrillar Crystalline Superstructure: Achieving High-Performance Polylactide. *ACS Appl. Mater. Interfaces* **2017**, *9*, 25818–25829. [[CrossRef](#)]
40. Fambri, L.; Pegoretti, A.; Fenner, R.; Incardona, S.D.; Migliaresi, C. Biodegradable fibres of poly(l-lactic acid) produced by melt spinning. *Polymer* **1997**, *38*, 79–85. [[CrossRef](#)]
41. Puchalski, M.; Kwolek, S.; Szparaga, G.; Chrzanowski, M.; Krucińska, I. Investigation of the Influence of PLA Molecular Structure on the Crystalline Forms (α' and α) and Mechanical Properties of Wet Spinning Fibres. *Polymers* **2017**, *9*, 18. [[CrossRef](#)]
42. Puchalski, M.; Krucińska, I.; Sulak, K.; Chrzanowski, M.; Wrzosek, H. Influence of the calender temperature on the crystallization behaviors of polylactide spun-bonded non-woven fabrics. *Text. Res. J.* **2013**, *83*, 1775–1785. [[CrossRef](#)]
43. Bhat, G.; Gulgunje, P.; Desai, K. Development of structure and properties during thermal calendaring of polylactic acid (PLA) fiber webs. *Express Polym. Lett.* **2008**, *2*, 49–56. [[CrossRef](#)]
44. Alex, A.; Ilango, N.K.; Ghosh, P. Comparative Role of Chain Scission and Solvation in the Biodegradation of Polylactic Acid (PLA). *J. Phys. Chem. B* **2018**, *122*, 9516–9526. [[CrossRef](#)] [[PubMed](#)]
45. Harris, A.M.; Lee, E.C. Heat and humidity performance of injection molded PLA for durable applications. *J. Appl. Polym. Sci.* **2010**, *115*, 1380–1389. [[CrossRef](#)]
46. Yu, L.; Liu, H.; Xie, F.; Chen, L.; Li, X. Effect of annealing and orientation on microstructures and mechanical properties of polylactic acid. *Polym. Eng. Sci.* **2008**, *48*, 634–641. [[CrossRef](#)]
47. Zhou, C.; Li, H.; Zhang, W.; Li, J.; Huang, S.; Meng, Y.; Christiansen, J.d.; Yu, D.; Wu, Z.; Jiang, S. Direct investigations on strain-induced cold crystallization behavior and structure evolutions in amorphous poly(lactic acid) with SAXS and WAXS measurements. *Polymer* **2016**, *90*, 111–121. [[CrossRef](#)]
48. Yousefzade, O.; Jeddi, J.; Franco, L.; Puiggali, J.; Garmabi, H. Crystallization kinetics of chain extended poly(L-lactide)s having different molecular structures. *Mater. Chem. Phys.* **2020**, *240*, 122217. [[CrossRef](#)]
49. Ghazaryan, G.; Schaller, R.; Feldman, K.; Tervoort, T.A. Rejuvenation of PLLA: Effect of plastic deformation and orientation on physical ageing in poly(l-lactic acid) films. *J. Polym. Sci. Part B Polym. Phys.* **2016**, *54*, 2233–2244. [[CrossRef](#)]
50. Taubner, V.; Shishoo, R. Influence of processing parameters on the degradation of poly(L-lactide) during extrusion. *J. Appl. Polym. Sci.* **2001**, *79*, 2128–2135. [[CrossRef](#)]
51. Yuniarto, K.; Purwanto, Y.A.; Purwanto, S.; Welt, B.A.; Purwadaria, H.K.; Sunarti, T.C. Infrared and Raman studies on polylactide acid and polyethylene glycol-400 blend. *AIP Conf. Proc.* **2016**, *1725*, 020101.
52. Chen, H.-m.; Shen, Y.; Yang, J.-h.; Huang, T.; Zhang, N.; Wang, Y.; Zhou, Z.-w. Molecular ordering and α' -form formation of poly(l-lactide) during the hydrolytic degradation. *Polymer* **2013**, *54*, 6644–6653. [[CrossRef](#)]
53. Braun, B.; Dorgan, J.R.; Dec, S.F. Infrared Spectroscopic Determination of Lactide Concentration in Polylactide: An Improved Methodology. *Macromolecules* **2006**, *39*, 9302–9310. [[CrossRef](#)]
54. Meaurio, E.; Zuza, E.; Lopez-Rodriguez, N.; Sarasua, J.R. Conformational Behavior of Poly(l-lactide) Studied by Infrared Spectroscopy. *J. Phys. Chem. B* **2006**, *110*, 5790–5800. [[CrossRef](#)]
55. Stoclet, G.; Seguela, R.; Lefebvre, J.M.; Rochas, C. New Insights on the Strain-Induced Mesophase of Poly(d,l-lactide): In Situ WAXS and DSC Study of the Thermo-Mechanical Stability. *Macromolecules* **2010**, *43*, 7228–7237. [[CrossRef](#)]
56. Xue, B.; Xie, L.; Zhang, J. Detailed molecular movements during poly(l-lactic acid) cold-crystallization investigated by FTIR spectroscopy combined with two-dimensional correlation analysis. *RSC Adv.* **2017**, *7*, 47017–47028. [[CrossRef](#)]
57. Di Liso, V.; Sturabotti, E.; Francolini, I.; Piozzi, A.; Martinelli, A. Effects of annealing above T_g on the physical aging of quenched PLLA studied by modulated temperature FTIR. *J. Polym. Sci. Part B Polym. Phys.* **2019**, *57*, 174–181. [[CrossRef](#)]
58. Vyavahare, O.; Ng, D.; Hsu, S.L. Analysis of Structural Rearrangements of Poly(lactic acid) in the Presence of Water. *J. Phys. Chem. B* **2014**, *118*, 4185–4193. [[CrossRef](#)] [[PubMed](#)]